AD-A171 863 THE ERODING FOIL SWITCH (EFS) MODEL(U) MISSION RESEARCH 1/1
CORP ALEXANDRIA VA J E BRANDENBURG ET AL. 01 JAN 86
MRC/WDC-R-103 DNA-TR-86-83 DNA001-84-C-0208

UNCLASSIFIED F/G 10/2 NL

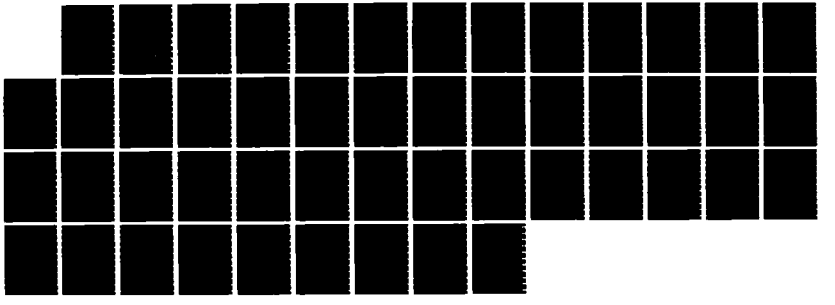

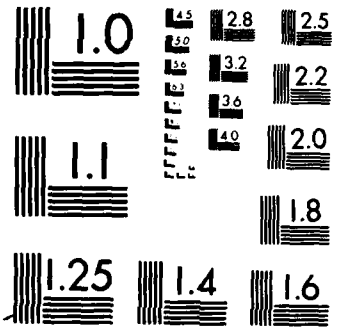
1.0
1.1
1.25
1.4
1.6
1.8
2.0
2.2
2.5
2.8
3.2
3.6
4.0

DNA-TR-86-83

THE ERODING FOIL SWITCH (EFS) MODEL

John E. Brandenburg
Mission Research Corporation
5503 Cherokee Avenue
Alexandria, VA 22312

1 January 1986

Technical Report

CONTRACT No. DNA 001-84-C-0208

THIS WORK WAS SPONSORED BY THE DEFENSE NUCLEAR AGENCY
UNDER RDT&E RMSS CODE B323085466 T99QMXLA00013 H2590D.

Prepared for
Director
DEFENSE NUCLEAR AGENCY
Washington, DC 20305-1000

Destroy this report when it is no longer needed. Do not return to sender.

PLEASE NOTIFY THE DEFENSE NUCLEAR AGENCY, ATTN: STTI, WASHINGTON, DC 20305-1000, IF YOUR ADDRESS IS INCORRECT, IF YOU WISH IT DELETED FROM THE DISTRIBUTION LIST, OR IF THE ADDRESSEE IS NO LONGER EMPLOYED BY YOUR ORGANIZATION.

DISTRIBUTION LIST UPDATE

This mailer is provided to enable DNA to maintain current distribution lists for reports. We would appreciate your providing the requested information.

☐ Add the individual listed to your distribution list.

☐ Delete the cited organization/individual

☐ Change of address.

NAME: _____

ORGANIZATION: _____

OLD ADDRESS	CURRENT ADDRESS
_____	_____
_____	_____
_____	_____

TELEPHONE NUMBER: (___) _____

SUBJECT AREA(s) OF INTEREST:

_____	_____
_____	_____
_____	_____

DNA OR OTHER GOVERNMENT CONTRACT NUMBER: _____

CERTIFICATION OF NEED-TO-KNOW BY GOVERNMENT SPONSOR (if other than DNA):

SPONSORING ORGANIZATION: _____

CONTRACTING OFFICER OR REPRESENTATIVE: _____

SIGNATURE: _____

Director
Defense Nuclear Agency
ATTN: STTI
Washington, DC 20305-1000

Director
Defense Nuclear Agency
ATTN: STTI
Washington, DC 20305-1000

UNCLASSIFIED

SECURITY CLASSIFICATION OF THIS PAGE AD-A171562

REPORT DOCUMENTATION PAGE

Form Approved
OMB No. 0704-0188
Exp. Date: Jun 30, 1986

1a. REPORT SECURITY CLASSIFICATION UNCLASSIFIED	1b. RESTRICTIVE MARKINGS
2a. SECURITY CLASSIFICATION AUTHORITY N/A since Unclassified	3. DISTRIBUTION/AVAILABILITY OF REPORT Approved for public release; distribution is unlimited.
2b. DECLASSIFICATION/DOWNGRADING SCHEDULE N/A since Unclassified	
4. PERFORMING ORGANIZATION REPORT NUMBER(S) MRC/WDC-R-103	5. MONITORING ORGANIZATION REPORT NUMBER(S) DNA-TR-86-83
6a. NAME OF PERFORMING ORGANIZATION Mission Research Corporation 6b. OFFICE SYMBOL (If applicable)	7a. NAME OF MONITORING ORGANIZATION Director Defense Nuclear Agency
6c. ADDRESS (City, State, and ZIP Code) 5503 Cherokee Avenue Alexandria, Virginia 22312	7b. ADDRESS (City, State, and ZIP Code) Washington, DC 20305-1000
8a. NAME OF FUNDING/SPONSORING ORGANIZATION 8b. OFFICE SYMBOL (If applicable)	9. PROCUREMENT INSTRUMENT IDENTIFICATION NUMBER DNA 001-84-C-0208
8c. ADDRESS (City, State, and ZIP Code)	10. SOURCE OF FUNDING NUMBERS PROGRAM ELEMENT NO. 62715H; PROJECT NO. T99QMXL; TASK NO. A; WORK UNIT ACCESSION NO. DH008390

11. TITLE (Include Security Classification)
THE ERODING FOIL SWITCH (EFS) MODEL

12. PERSONAL AUTHOR(S)
Brandenburg, John E., Mission Research Corporation and Terry, Robert E., Naval Research Lab

13a. TYPE OF REPORT	13b. TIME COVERED	14. DATE OF REPORT (Year, Month, Day)	15. PAGE COUNT
Technical Report	FROM 850930 TO 851231	860101	48

16. SUPPLEMENTARY NOTATION This work was sponsored by the Defense Nuclear Agency under RDT&E RMSS Code B323085466 T99QMXLA00013 H2590D.

17. COSATI CODES		
FIELD	GROUP	SUB-GROUP
9	5	
10	2	

18. SUBJECT TERMS (Continue on reverse if necessary and identify by block number)
Pulse Power; Eroding Foil Switch; Capacitor Banks; EFS

19. ABSTRACT (Continue on reverse if necessary and identify by block number)

An analysis of the results of two experiments, the Los Alamos Foil Switch Experiment and the Magnetic Gate Experiment, reveals evidence of mass loss and unexpectedly high temperatures in strongly accelerated aluminum foils. Nonlinear magnetic diffusion theory is analyzed both analytically and numerically and found to give strong concentrations of current density, in a propagating front, for foils thicker than a classical skin depth. This concentrated current front is found to lead to mass erosion and high temperatures in foils undergoing strong acceleration. These results are used to formulate a new model of foil kinematics called the EFS model that features both a "rocket" (or mass loss) phase, and a "snowplow" (shock wave) phase after foil disassembly. This model is shown to give good agreement with experimental results.

20. DISTRIBUTION/AVAILABILITY OF ABSTRACT	21. ABSTRACT SECURITY CLASSIFICATION
☐ UNCLASSIFIED/UNLIMITED ☒ SAME AS RPT. ☐ DTIC USERS	UNCLASSIFIED
22a. NAME OF RESPONSIBLE INDIVIDUAL Betty L. Fox	22b. TELEPHONE (Include Area Code) (202) 325-7042 22c. OFFICE SYMBOL DNA/STTI

DD FORM 1473, 84 MAR 83 APR edition may be used until exhausted. All other editions are obsolete.

SECURITY CLASSIFICATION OF THIS PAGE
UNCLASSIFIED

PREFACE

The authors are grateful for useful discussions with Dr. Bruce Goplen of Mission Research and Dr. John Ambrosiano of Berkeley Research Associates. In addition, particular thanks is made to Dr. N. R. Pereira of Berkeley Research Associates for his valuable comments concerning the effects of nonlinear magnetic diffusion.

TABLE OF CONTENTS

Section		Page
	PREFACE	iii
	LIST OF ILLUSTRATIONS	v
1	INTRODUCTION	1
	1.1 The Foil Switch Problem	1
	1.2 The Foil Switch	1
	1.3 Report Overview and Motivation	3
2	SWITCH EXPERIMENTS	5
	2.1 The Foil Switch Experiment	5
	2.2 The Magnetic Gate Experiment	7
	2.3 The Interpretation of Experimental Data	10
3	THE PHYSICS OF THE EFS MODEL	14
	3.1 Nonlinear Magnetic Diffusion: Numerical and Approximate Treatments	14
	3.2 Nonlinear Magnetic Diffusion: The Equipartition Approximation	19
	3.3 Mass Erosion and Magnetic Acceleration: The Rocket Equation	22
	3.4 Mass Erosion Coupled with Mass Grading	24
	3.5 Approximations and Problems Associated with Mass Erosion	25
	3.6 Foil Motion After Erosion: The Snowplow Equation	26
	3.7 Discussion	28
4	THE EFS MODEL OF FOIL MOTION	29
	4.1 The "Rocket" and "Snowplow" Phases of EFS	29
	4.2 Interpretation of the LANL Foil Switch Results	30
5	DISCUSSION	33
6	LIST OF REFERENCES	35

LIST OF ILLUSTRATIONS

Figure		Page
1	A Diagram of the LANL Foil Switch Experiment	2
2	Plot of Normalized Switched Current (Switched Current Divided by Bank Current) for Los Alamos Foil Switch Experiment	8
3	A Diagram of the Magnetic Gate Experiment	9
4	Current Versus Time for the Magnetic Gate Switch Experiment	11
5	A Plot of Foil Position Versus Time From the Magnetic Gate Experiment	12
6	Plots of Various Quantities in Normalized Units Versus Normalized Distance from the Numerical Solution of the Nonlinear Diffusion Problem	16
7	A Plot of Velocity Versus Time for the EFS Model Calculation of the Los Alamos Foil Switch Experiment	32

SECTION 1
INTRODUCTION

1.1 THE FOIL SWITCH PROBLEM.

The Eroding Foil Switch (EFS) model describes foil motion in a foil switch. The foil switch is a promising concept for sharpening the risetime and thus increasing the power of capacitor banks used in pulsed power applications.[1] This report describes both the foil switch device and experimental results obtained with it. The EFS model will be derived and shown to provide a reasonable explanation of experimental results. The EFS model will also be shown to suggest methods of improving switch performance.

1.2 THE FOIL SWITCH.

A foil switch consists of a coaxial transmission line with a thin annular foil mounted between the inner and outer electrodes (Figure 1). When a voltage is applied by a capacitor bank to the electrodes, current flows in the foil, and a Lorentz force pushes the foil down the transmission line. A gap in the outer electrode of the line allows rapid switching of current when the foil passes. The load that the current is to be switched into is connected across the gap, so that the passage of the foil across the gap will suddenly introduce the load into the circuit.

Three important effects must be considered when designing a foil switch:

1) The foil should reach the gap at high velocity so that the switching time,

$$\Delta t = d/V_f \quad , \tag{1.1}$$

where d is the gap width and V_f is the foil velocity at the gap, is as short as possible.

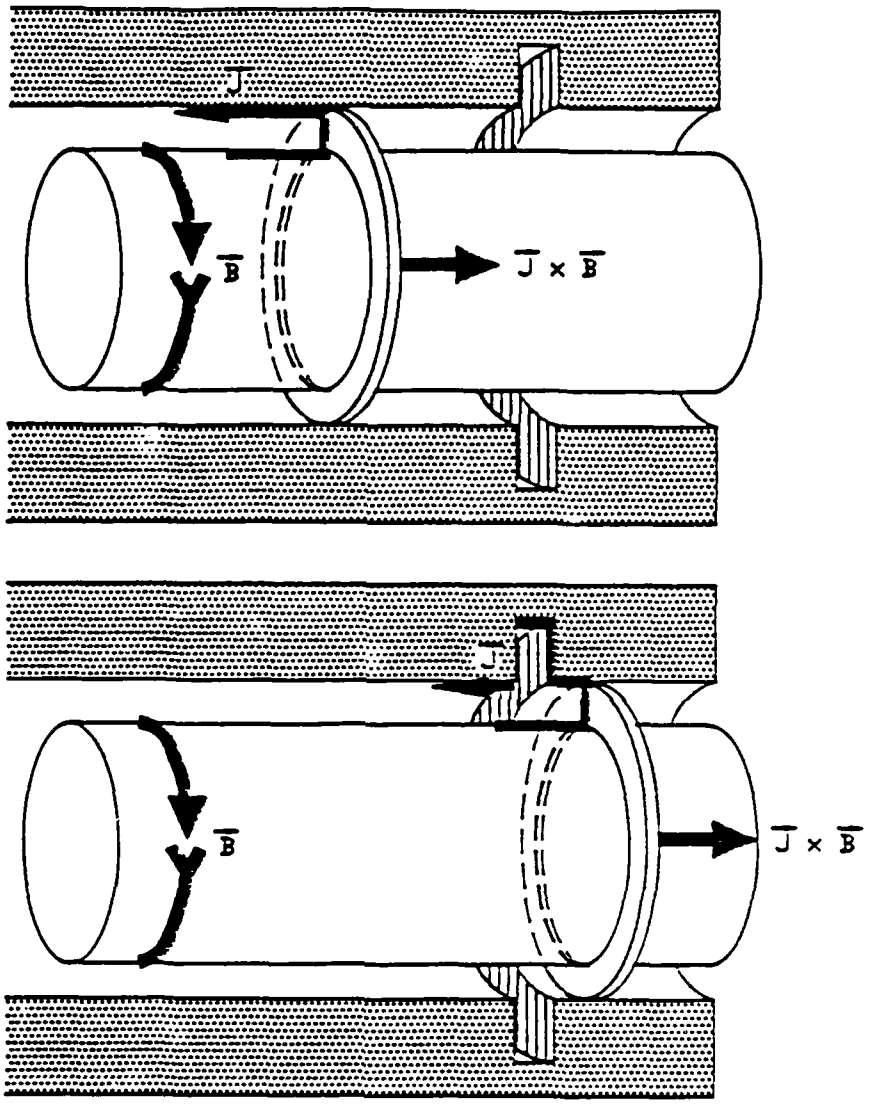

Figure 1. A diagram of the LANL foil switch experiment.

2) The gap must be kept clear of both foil fragments and plasma, so that it will not "short out," allowing current to bypass the load. This requirement of a "clean gap" means that the foil must be shaped so that it accelerates in one piece rather than fragmenting due to unequal magnetic forces. It also requires that the foil not be too light, or it will vaporize due to resistive heating before it reaches the gap, filling the gap with vapor.

3) The foil motion must be calculated to allow the foil to reach the gap at the time of maximum current, that is, the quarter cycle time of the bank. The inductance of the switch is usually chosen to be much less than the inductance of the load or the driving circuit, so that the bank waveform is unaffected by the foil motion.

1.3 REPORT OVERVIEW AND MOTIVATION.

The optimum design of a foil switch requires understanding of the foil motion and heating. The same currents that accelerate the foil will also heat it. Therefore, the requirements of high foil velocity and no foil vaporization must be balanced against one another. The foil equation of motion also determines the choice of gap placement in the transmission line, so that the foil can arrive at the gap at the time of maximum bank current. Present models[1,2] of foil motion assume uniform heating and constant mass for the foil. These models, however, appear inadequate when their predictions are compared with experimental data. The foils appear to reach a much higher temperature than is predicted using a uniform current model and to arrive at the gap earlier than expected using constant mass.

A new model for foil motion, which is far more consistent with experimental data, has been formulated. This model is called the Eroding Foil Switch (EFS). The EFS model assumes two phases of foil motion: an initial "rocket" phase and a secondary "snowplow" phase. The EFS model assumes that, initially, currents in an accelerated foil flow in a thin

layer rather than uniformly. This effect, due to nonlinear magnetic diffusion, results in ablation or erosion in thin layers of the foil as it accelerates. This is called the "rocket" phase because the mass of the foil becomes smaller as it accelerates. The mass decreases at a rate proportional to the resistive heating. Therefore, the foils in this model arrive at the switching gap much sooner than is predicted by constant mass models. The erosion of the foil can lead to its complete disassembly. The magnetic field pushing the foil then diffuses through the exploded foil as a shock wave. This is called the "snowplow" phase.

In the body of this report, we will first discuss the experimental data that first suggested the EFS model. A derivation of the equations of motion of two phases of the EFS model will then be shown. Finally, the EFS model will be applied to the results of a foil switch experiment.

SECTION 2
SWITCH EXPERIMENTS

2.1 THE FOIL SWITCH EXPERIMENT.

The EFS model is based on the results of two experiments. The most important of these experiments is the foil switch. The foil switch experiment[1] consisted of a coaxial transmission line of two electrodes (Figure 1). The inner electrode had an 0.8 cm radius and an outer electrode which formed a sleeve with an inner surface radius of 1.1 cm. The annular cavity thus formed had a height of 0.3 cm. In this cavity, an annular foil of 0.3 cm height and 0.07 cm average thickness was mounted. A gap 0.3 cm wide was cut in the outer electrode beginning 1.0 cm from the mounting point of the foil.

Because a variation of magnetic force occurred on the foil due to the radial variation of the magnetic field, the foil was "mass graded" in radius so that the mass per unit area, $\mu = \rho_o \delta$, where μ is the mass per unit area, ρ_o is the foil material mass density, and δ is the foil thickness, was proportional to the magnetic force per unit area on the foil, $B^2/8\pi$ (in cgs units), where B is the magnetic field strength. Assuming the mass per unit area, μ, was constant in time, the acceleration of each part of the foil was given,

$$\partial^2_t z = B^2(t,r)/(8\pi\mu(r)) \quad . \tag{2.1}$$

Where z is the distance in the direction of foil motion, the z axis, and B varies as 1/r, due to the coaxial geometry:

$$B = \frac{2I}{cr} \quad , \tag{2.2}$$

where I is the current, c is the speed of light, and r is the radius. The foil mass per unit area (or thickness, δ,) had to vary by approximately $1/r^2$

$$\partial_t^2 z = A(t) \quad , \tag{2.3}$$

that is, an acceleration that is constant in radius and moves each part of the foil equally. This mass grading is necessary because of the high accelerations experienced by the foil. These accelerations would create stresses exceeding the foil yield strength if they were not distributed equally. The foil mass and distance to the gap were also chosen carefully, assuming that the foil mass would remain constant.

The foil was heated by the electric current flowing in it and would melt and even vaporize if accelerated long enough. The experimental parameters were chosen so that the foil would only become molten (660°C) when it reached the gap. These calculations assumed, however, that the foil would heat uniformly.

The actual calculation of foil parameters, accelerations, and heating rates will only be summarized in this report but are calculated in detail in a companion report, *"Physical Properties and Numerical Models of Foils in High Current Switches."*[3]

The foil equation of motion, assuming the foil retained its original mass, is found (using the characteristic time, $\tau = 10^{-5}$sec, for convenience)

$$\partial_t V = 3.7\text{cm}/\tau^2(\sin^2\omega t) \quad , \tag{2.4a}$$

where $\omega = 2.8\tau^{-1}$. (2.4b)

The functions for z and V can be integrated and become

$$V = 1.85\text{cm}/\tau^2\left(t - \frac{1}{2\omega}\sin(2\omega t)\right) \tag{2.5a}$$

$$z = 1.85\text{cm}/\tau^2\left(t^2/2 + \frac{1}{2\omega^2}\sin^2(\omega t)\right) \quad . \tag{2.5b}$$

Similarly, the function for foil temperature is found to be

$$T(t) = 1.5 \times 10^7 \ C^o/sec \ (t - \frac{1}{2\omega} \sin(2\omega t)) \ . \qquad (2.6)$$

The results of the experiment were as follows. The foil apparently reached the gap in $t = 0.7\tau = 7x10^{-6}$sec and achieved a velocity of $V = 3.0cm/\tau = 3x10^5 cm/sec$. The foil reached the gap sooner than expected indicating 50% of its original mass may have been lost. The switch signal was a linear rise over 0.1τ (10^{-6} sec) (Figure 2), rather than a sharp rise consistent with a concentrated source of current. Temperature diagnostics showed that the foil had reached a 4000°C temperature rather than the expected 600°C. Therefore, the foil appeared to have lost mass as it accelerated and also to have heated more strongly than expected.

2.2 THE MAGNETIC GATE EXPERIMENT.

The magnetic gate experiment[2] was a switching experiment of different geometry from the foil switch. It yielded much data on foil motion, because the foil trajectory was more thoroughly diagnosed than in the foil switch experiment.

The magnetic gate experiment differed from the foil switch in many respects, chief of which was having several gaps instead of one. This provided data on the location of the foil at several points in time. The magnetic gate experiment also differed from the foil switch in that it was a linear transmission line rather than a coaxial system (Figure 3), and the foil being accelerated consisted of a thinned region of a larger metal gate, rather than a simple thin foil. The gate thickness was 0.2 cm, much thicker than the foil in the foil switch. The foil was driven by a capacitor bank delivering 2.5 MA peak current with a quarter cycle time of 4.8 microseconds.

The magnetic gate was designed to open by stretching out the thinned region when the magnetic pressure exceeded the yield strength of the gate. The thick portions of the gate would then bend down as hinges and

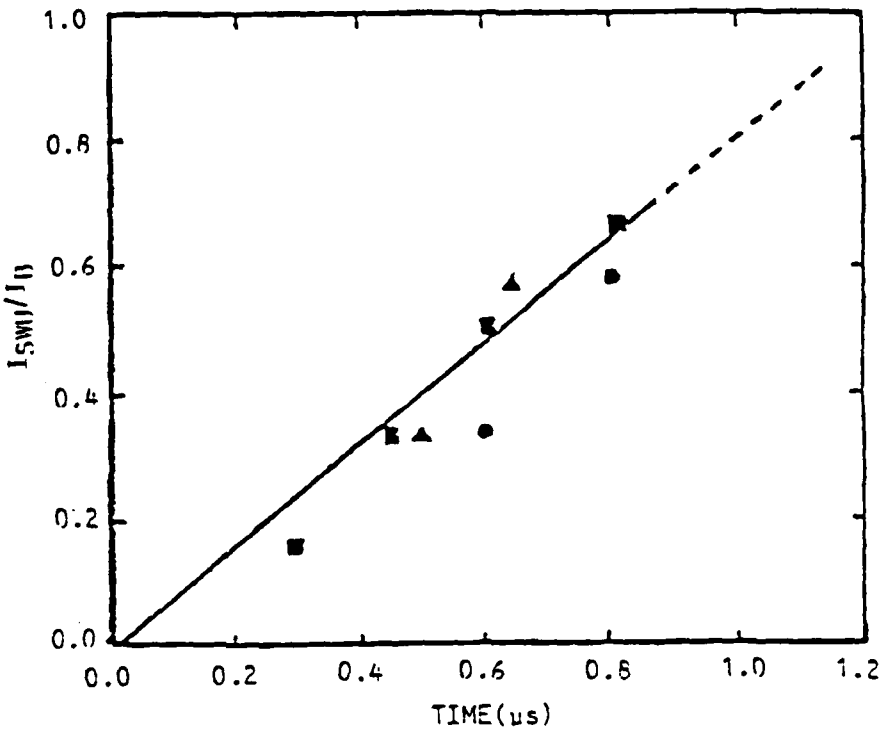

Figure 2. Plot of normalized switched current (switched current divided by bank current) for the Los Alamos foil switch experiment.

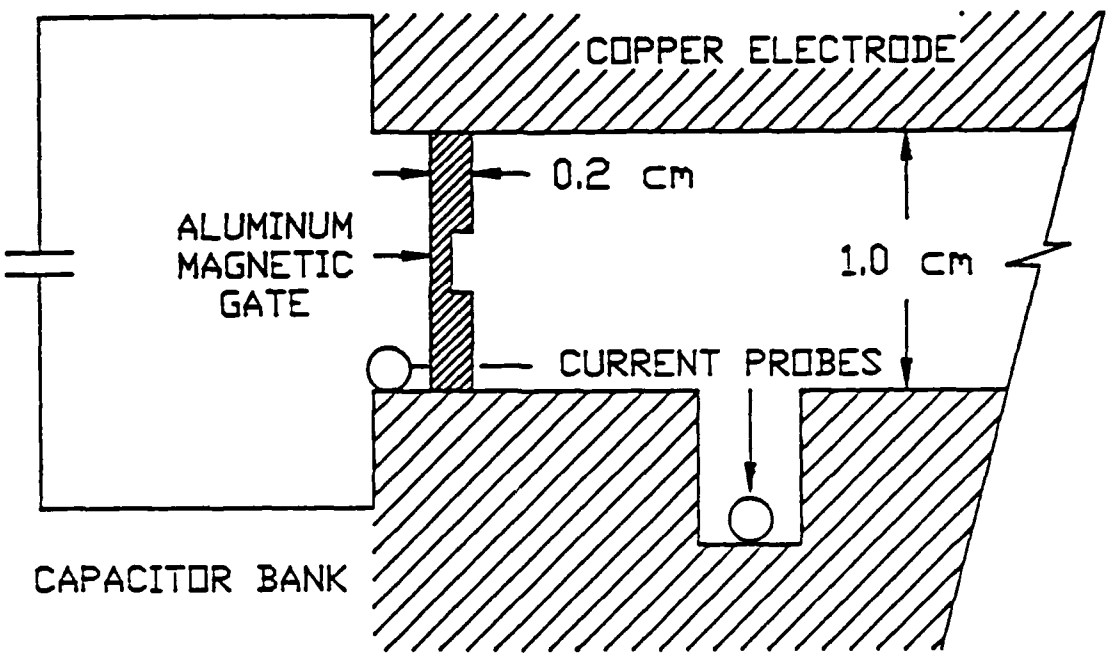

Figure 3. A diagram of the magnetic gate experiment.

allow the thin region to accelerate as a foil. The resulting current carrying foil switched the current through the gaps with very high efficiency, switching almost 100% of the bank current (Figure 4). However, the foil moved as if it had lost 95% of its original mass (Figure 5); the foil moved down the transmission line much more rapidly than anticipated. In particular, the last data point on the plot of foil position versus time indicates it is losing mass as it accelerates. This is because the last data point is above the curve fitting the first two points and thus indicating that it is moving faster than expected.

2.3 THE INTERPRETATION OF EXPERIMENTAL DATA.

Despite the differences between the foil switch and magnetic gate experiments, similar phenomena occurred in each. In both experiments, large mass losses were observed in the accelerated foils. In addition, foil heating was observed greatly in excess of what was expected from models of uniform current flow in the foils.

In the foil switch experiment, the kinematic results were consistent with roughly a 50% initial mass loss from the foil. However, an examination of the apparatus after the experiments revealed a continuous film of foil residue down the line, rather than any concentration of debris at the foil starting point that would indicate an abrupt initial mass loss.[4] The experimenters suggested viscous entrainment of foil material as a mechanism for mass loss.

The switch signal itself was not what one would expect from a concentrated current flowing in a foil. However, the switch current signal could be explained by a simple physical model. The model consisted of a region of uniform current density 1 cm wide that moved at uniform speed across the gap. The current density acted like a commutator brush to transfer current from one side of the gap to another. The switch current through the gap was then

$$I_s = J_o x \quad , \tag{2.7}$$

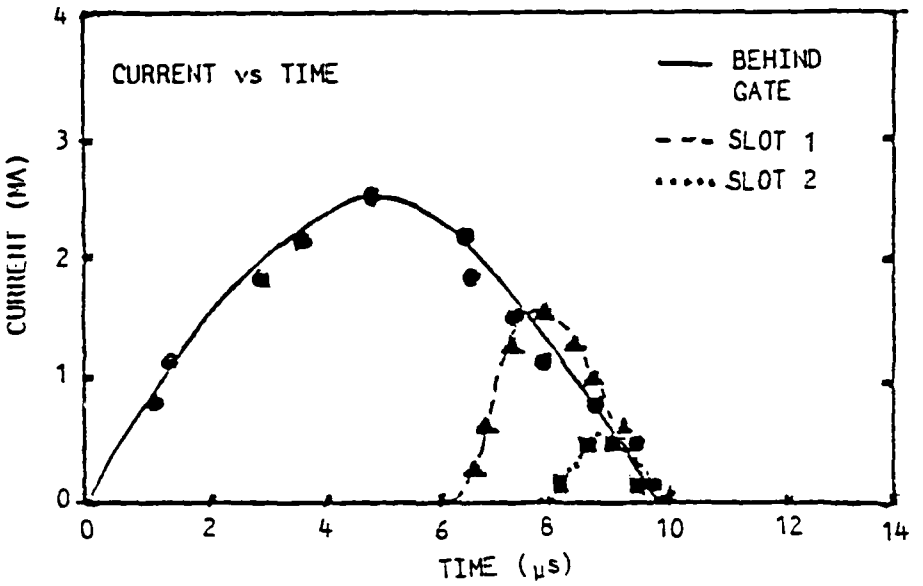

Figure 4. Current versus time for the magnetic gate switch experiment.

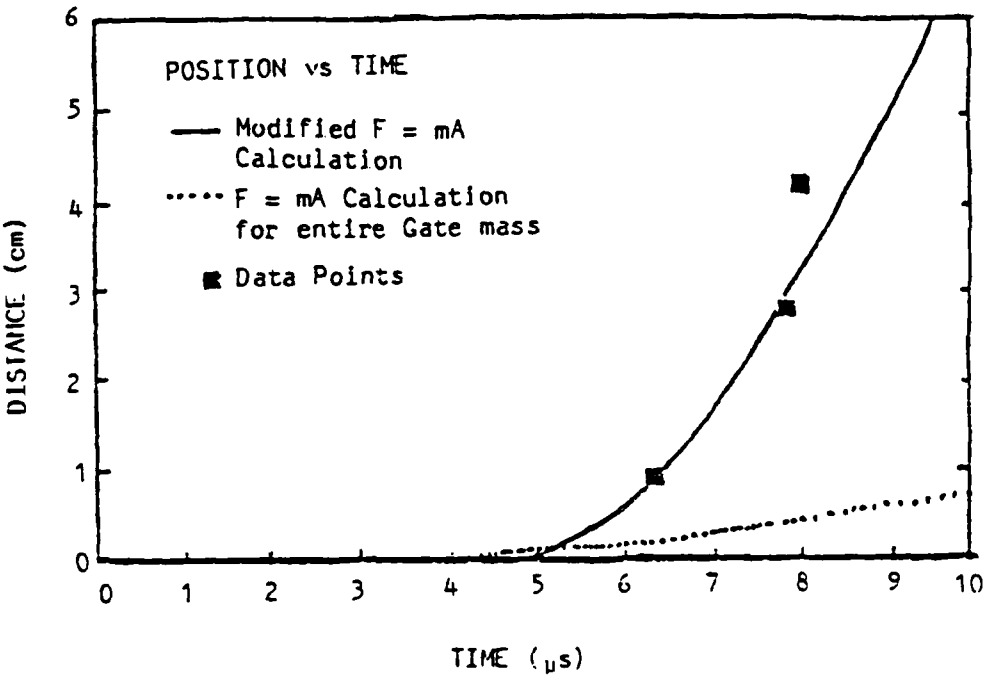

Figure 5. A plot of foil position versus time from the Magnetic Gate Experiment. (1) experiment data (squares), (2) F=ma calculations using the entire gate mass (dotted curve), (3) F=ma calculations using 5% of the original gate mass (solid curve).

where J_o is the current density in megaamps per cm; x is defined as

$$x = V_o t - d \quad , \tag{2.8}$$

where V_o is the uniform velocity, and d is the location of the far side of the gap. This expression obviously gives a linear rising current as is seen in the experiment. However, the uniform current is spread over a large (≈1 cm) area, which was much larger than the foil mean thickness at its starting point. If the model of a diffuse uniform current was correct, then the foil was no longer a dense object, but a vapor. This was consistent with optical pyrometry signals from the foil which indicated a 4000°C temperature. The foil had evidently vaporized. However, using the model that the foil would carry a uniform current and thus heat uniformly, the foil mass had been chosen to ensure that it would not reach such high temperatures.

In the magnetic gate experiment, a large mass loss was observed as in the foil switch experiment. In addition, the foil was observed to become incandescent, indicating high temperature, though precise temperature measurements were not made.

Therefore, the two experiments indicate that models of foil motion, which assume uniform current density and constant foil mass, are inadequate. A new model for foil motion allowing mass loss and rapid heating is needed. Such a model will now be derived based on a careful study of the flow of current in strongly accelerated foils. The effects of nonlinear magnetic diffusion and strong acceleration will be found to result in both mass loss and rapid heating of foils.

SECTION 3
THE PHYSICS OF THE EFS MODEL

In the previous section, we discussed the results of experiments on strongly accelerated foils. In both of these experiments, the mass of the foils appeared to decrease during acceleration, and the foils became much hotter than was expected. Both of these effects can be explained if current did not flow uniformly in the foil but instead concentrated in a small region which then moved through the foil.

If the current concentrated in a layer, thin compared to the thickness of the foil, the current would strongly heat the foil locally. Also, the force pushing the foil would be concentrated in this layer, and as the layer moved forward, it would "leave behind" heated foil material. The foil material behind the concentrated current would no longer be accelerated but would instead be under tension, and if accelerations were strong, would be torn off the foil in the form of small droplets. The foil mass would then decrease as the foil was accelerated.

In this section, the phenomenon of nonlinear magnetic diffusion will be shown to lead to concentration of current in a thin foil. The effects of this current concentration will be shown to lead to mass erosion in strongly accelerated foils. The effect of mass erosion on the foil equation of motion will then be discussed. This erosion can consume the foil completely. The foil material will then explode into vapor with the magnetic field moving through it as a shock wave. The EFS model is then seen to arise easily from these concepts. The EFS model can be said to be the kinematics of light foils undergoing nonlinear magnetic diffusion.

3.1 NONLINEAR MAGNETIC DIFFUSION: NUMERICAL AND APPROXIMATE TREATMENTS.

When a magnetic field is applied to any conductor, all current initially is in a thin layer on the conductor surface. As time progresses, the current layer broadens and fills the conductor interior. The concentration of current in a thin layer will result in a strong ohmic heating rate,

$$\partial_t Q = \eta J^2 \quad , \tag{3.1}$$

where Q is the thermal energy per unit volume in ergs/cm^3, J is the electric current density,

$$J = \frac{c}{4\pi} \partial_z B \quad , \tag{3.2}$$

from Amperes law in our geometry, and η is the resistivity in seconds (cgs units). In general, η is a function of Q,

$$\eta = \eta_0 + C_1 Q + C_2 Q^2 \ldots \tag{3.3}$$

The constants C_1 and C_2 were chosen to fit a curve in reference 5. They were given the values

$$C_1 = 4.8\times10^{-24} \text{ sec/bar and } C_2 = 3.9\times10^{-24} \text{ sec/bar}^2$$

by the authors for the purposes of numerical calculations.

Ignoring radial variations, we can write using Faraday's, Ohm's, and Ampere's laws,

$$\partial_t B = \frac{c^2}{4\pi} \partial_z(\eta \partial_z B) \quad . \tag{3.4}$$

Realistic resistivity models[5] were employed for Equations 3.1, 3.3, and 3.4, which were solved as a coupled system. Results for a magnetic field-foil system similar to the experiment (Figure 6) showed the current forming a layer and propagating as a wave through the system. Since JxB forces would be concentrated in this layer, the metal left behind by the current layer passage would no longer be pushed by the magnetic pressure and thus be left behind (assuming that being heated, it would lose its material strength under these conditions and slough or spall off in droplets).

Analytically, the advance of the diffusion wave can be understood by studying the set of Equations 3.1 - 3.4 and making some physically reasonable approximations. A more general approximate treatment of this problem is given in the next section of this report; also, an extensive discussion of this effect is given in Reference 6.

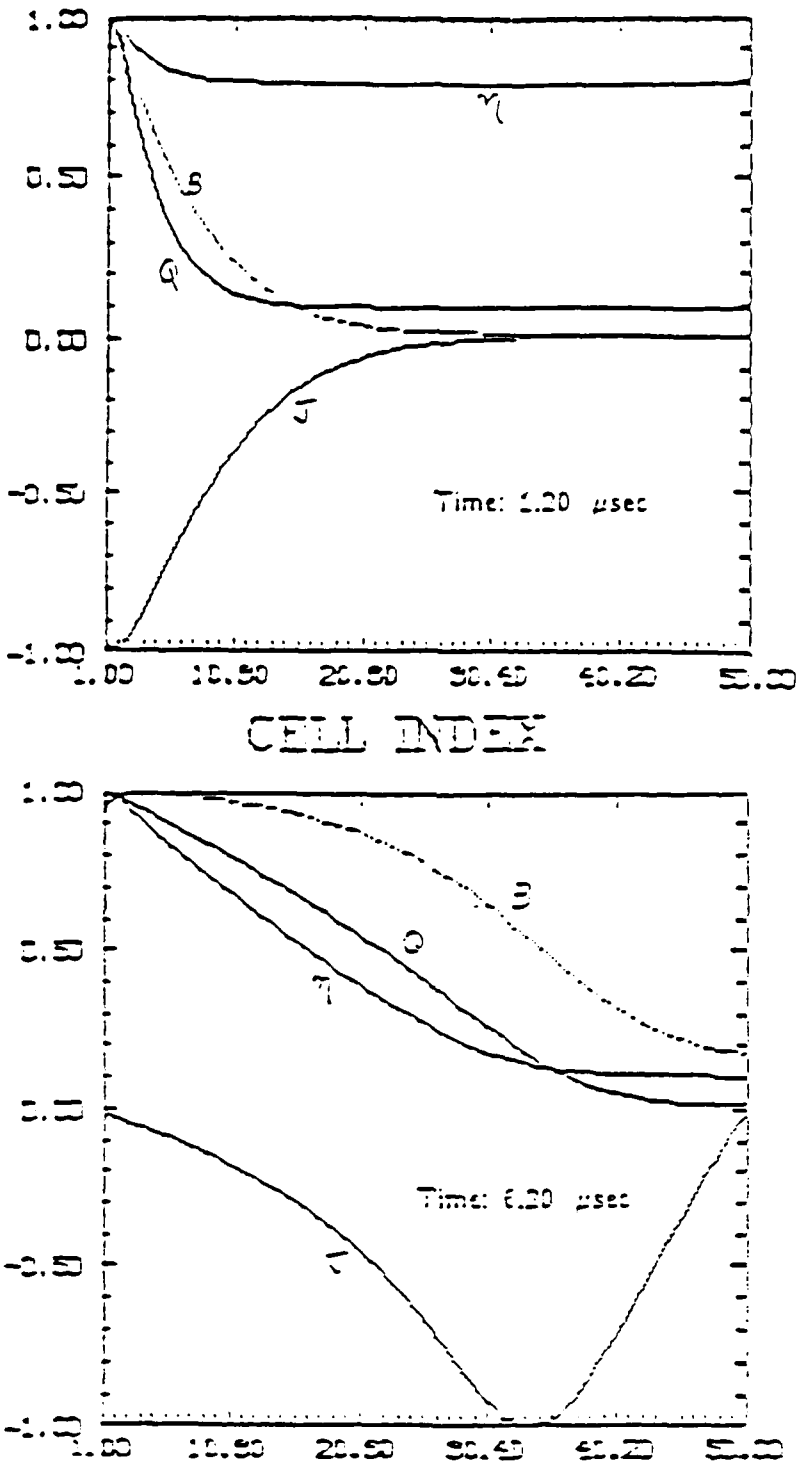

Figure 6. Plots of various normalized quantities versus normalized distance from the numerical solution of the nonlinear diffusion problem. Quantities shown are normalized: B, magnetic field; J, current density; η, resistivity; and Q, thermal energy density. Plots are for two times.

The current begins as a thin layer decaying exponentially into the unheated metal with a characteristic length of a "skin depth,"

$$J = J_o e^{z/\zeta} \quad , \quad \zeta = \left(\frac{2c^2 \eta_o}{4\pi\omega}\right)^{1/2} \quad , \tag{3.5}$$

where ω is the field frequency or inverse rise time. As the metal heats due to the skin current, it will become more resistive, and the current will also diffuse more deeply into the metal. The current will now decay behind the layer of peak current density, because the resistivity will be high. The current will thus concentrate where resistivity is just beginning to rise in the metal. In this region, the resistivity will be nearly linear in internal energy,[4] so that Equation 3.3 reduces to:

$$\eta \approx \eta_o + C_1 Q \quad . \tag{3.6}$$

We can thus write for Equation 3.1:

$$\partial_t \eta = C_1 \eta J^2 \quad . \tag{3.7}$$

We also consider this effect of a peak in current density in the region of small increase in resistivity: in the region of interest, the magnetic field will increase strongly, but then assume nearly the value it has on the boundary. In the region of interest, where the diffusion wave is actually advancing, we have a peak of current,

$$\partial_z J \approx 0 \quad , \tag{3.8a}$$

which means:

$$\partial_z^2 B \approx 0 \quad . \tag{3.8b}$$

We can then write for Equation 3.4

$$\partial_t B \simeq \frac{c^2}{4\pi} \partial_z \eta \, \partial_z B \quad . \tag{3.9}$$

This equation describes a convection of B across the system in a self-similar manner at a speed:

$$V_B = \frac{c^2}{4\pi} \partial_z \eta \quad . \tag{3.10}$$

We now can solve for this speed by solving Equations 3.7 and 3.9 together

$$\partial_t \eta = \partial_B \eta \partial_t B = \frac{c^2 C_\perp}{(4\pi)^2} (\partial_z B)^2 \quad , \tag{3.11a}$$

assuming η and Q are functions of B:

$$\partial_B \eta \partial_z \eta \partial_z B = \frac{C_\perp \eta (\partial_z B)^2}{4\pi} \quad , \tag{3.11b}$$

which simplifies to:

$$(\partial_z \eta)^2 = \frac{C_\perp \eta}{4\pi} (\partial_z B)^2 \quad . \tag{3.11c}$$

Integration in z over the region of linear behavior gives

$$\eta = \frac{C_\perp B^2}{8\pi} \quad . \tag{3.12}$$

This relation can be rewritten:

$$\Delta Q = \Delta B^2 / 8\pi \quad . \tag{3.13}$$

This condition will be called "Equipartition" and indicates, that in the region of important dynamics of the system, the magnetic and thermal energy densities couple at just the right rate to balance each other. That is, energy density changes are shared equally. This follows as the result of the approximations in the region of dynamics given by Equations 3.6 and 3.7. The Equipartition of energies is an interesting physical result that may be more general than the approximations used to find it. When

Equipartition is used itself as an initial assumption, it is found to allow great simplification of the nonlinear diffusion problem. This approach will be discussed in the next section.

3.2 NONLINEAR MAGNETIC DIFFUSION: THE EQUIPARTITION APPROXIMATION.

We attempt to find a general solution for the nonlinear magnetic diffusion problem that is insensitive to the exact dependence of resistivity, η, on the thermal energy density, Q, providing that η is monotonically increasing with Q.

We find this general solution for magnetic diffusion by making an approximation that is consistent with the case of a linear resistivity function.[5] The approximation used to find a general solution can be termed an "Equipartition Approximation;" that is, energy in the system should tend to divide itself equally into magnetic and thermal energies. Therefore, we should have generally:

$$B^2/8\pi = Q \quad . \tag{3.14}$$

This can be seen to be a reasonable assumption by Poyntings Theorem in the limit of negligible foil motion:

$$\partial_t(B^2/8\pi + Q) = \frac{c}{4\pi}\,\partial_z(EB) \quad , \tag{3.15}$$

which indicates that both magnetic and thermal energy densities can be lumped together with one source term. The suggestion that the source term would supply both energy densities equally seems an obvious one.

Keeping this approximation in mind, we can write both the magnetic diffusion equation and the heating equation in terms of the electric field, E, through Ohm's law,

$$E = \eta J \tag{3.16}$$

and Ampere's law,

$$E = \frac{c\eta}{4\pi} \partial_z B \quad . \tag{3.17}$$

Writing the magnetic equation, Equation 3.4, as:

$$\partial_t B = -c\, \partial_z E \quad , \tag{3.18}$$

and heating equation, Equation 3.1, as:

$$\partial_t Q = \frac{c}{4\pi} E \partial_z B \quad , \tag{3.19}$$

we can use our Equipartition Approximation to eliminate Q and use Equation 3.18 to write for Equation 3.19:

$$\frac{B}{4\pi} c\partial_z E = \frac{c}{4\pi} E \partial_z B \quad . \tag{3.20}$$

We can thus find the relation:

$$\ln E = \ln B + \ln L(t) \tag{3.21}$$

which becomes

$$E = L(t)B \quad , \tag{3.22}$$

where L(t) is a function of time only. Because E contains the resistivity, the exact form of the resistivity is not important as long as η rises with Q.

We can then write for Equation 3.18:

$$\partial_t B = -L(t)\partial_z B \quad . \tag{3.23}$$

The Equipartition Approximation has therefore allowed us to take the general nonlinear diffusion problem and reduce it to a linear, first order differential equation for B. Equation 3.22 is merely the equation for the translation of B at a speed L(t). Defining

$$z_o(t) = \int_o^t L(t')dt' \quad , \tag{3.24}$$

we can write

$$B = B_o F(z_o(t) - z) \tag{3.25}$$

where F is defined through

$$F(z_o(t)) = \frac{B(t)}{B_o} \Big| z = 0 \tag{3.26}$$

consistent with our less general treatment,

$$L(t) = \gamma \frac{B^2}{8\pi}(t) \quad . \tag{3.27}$$

We obtain for a sinusoidal magnetic field:

$$z_o(t) = \frac{\gamma}{2} \frac{B_o^2}{8\pi} \left(t - \frac{\sin 2\omega t}{2\omega}\right) \quad . \tag{3.28}$$

We also can obtain an approximate solution following Knoepfel[5] by assuming linear resistivity and Equipartition and the approximation that

$$B = B_o \ (\tau/\zeta)^{1}/^{2} \tag{3.29a}$$

with

$$\tau = V_B t - z \tag{3.29b}$$

with V_B a constant. It follows that

$$V_B = \frac{c^2 C_\perp}{8\pi \ell} \frac{B_o^2}{8\pi} \quad , \tag{3.30}$$

where ℓ is the characteristic length over which B varies in the region of sharp increase. In order for the two approximate treatments to agree asymptotically, we must have for γ in Equation 3.27:

$$\gamma = \frac{c^2 C_1}{4\pi \ell} \quad . \tag{3.31}$$

The diffusion wave speed depends on the magnetic field strength squared and thus the resistive heating rate. The diffusion wave velocity will then be approximately,

$$V_B = \frac{c^2}{4\pi} \partial_z \eta = \frac{c^2 C_1 B^2(t)}{32\pi^2 \zeta} \quad . \tag{3.32}$$

where we assume $\ell = \zeta/2$.
Using $\zeta = 0.04$ cm, $C_1 = 4.8 \times 10^{-21}$ sec/bar, we obtain

$$V_B = \frac{8\text{cm}}{\text{sec-bar}} \quad \frac{B_o^2}{8\pi} \quad . \tag{3.33}$$

where B_o is the magnetic field at the boundary and where a bar is 10^6 ergs/cm^3. This compares very favorably with the value obtained from numerical solution of Equations 3.1 through 3.4.

$$V_B = \frac{10 \text{ cm}}{\text{sec-bar}} \quad \frac{B_o^2}{8\pi} \quad . \tag{3.34}$$

These values will vary weakly with ω through ζ, however, given that ω varies only slightly between experiments $\zeta = .04$cm can be considered a constant.

3.3 MASS EROSION AND MAGNETIC ACCELERATION: THE "ROCKET" EQUATION.

The nonlinear magnetic diffusion will lead to mass erosion in strongly accelerated foils if the current layer formed is thin compared to the foil thickness. This must occur because the "magnetic pressure" or Lorentz force will push only that foil that is in front of the current layer. The foil material already heated, resistive, and passed by in the advance of the current layer will be torn away. This effect will only occur in thin foils undergoing high acceleration. Massive blocks of metal may only suffer

sloughing off of metal on long-time scales. The effect may also disappear in very thin foils where the current layer dimension is comparable to the thickness.

In a strongly accelerated foil the time derivitive of μ, the foil mass per unit area, is then:

$$\partial_t \mu = -\rho_o V_B \tag{3.35}$$

where ρ_o is the mass density of aluminum, 2.7 gm/cm^3.

We can define K:

$$\partial_t \mu = -K \frac{B^2(t)}{8\pi} \tag{3.36}$$

$$K = \rho_o \gamma$$

and evaluate it, approximately, using the value for V_B obtained analytically:

$$K \approx \frac{21 \text{gm}}{\text{cm}^2 \text{ sec-bar}} . \tag{3.37}$$

What then is the effect of mass erosion on foil equations of motion? The answer is found by solving the equations for motion for each part of the foil. For variable mass, Newton's law is written:

$$\partial_t(\mu V) = B^2/8\pi \quad . \tag{3.38}$$

We integrate Equation 3.38 in time:

$$\mu V = W(t) \quad , \tag{3.39}$$

where W(t) is an "action density,"

$$W(t) = \int B^2/8\pi \, dt \quad . \tag{3.40}$$

From Equation 3.36a we have for μ,

$$\partial_t \mu = -KB^2/8\pi \quad ; \tag{3.41}$$

we integrate both sides:

$$\mu = -KW(t) + \mu_o \quad , \tag{3.42}$$

where μ_o is the initial mass per unit area. We can write

$$\mu = \mu_o \left(1 - K \frac{W(t)}{\mu_o}\right) \quad . \tag{3.43}$$

We can then write for V:

$$V = \frac{W(t)}{\mu_o\left(1 - K \frac{W(t)}{\mu_o}\right)} \quad . \tag{3.44}$$

This is the equation for velocity in a system where mass erosion occurs at a rate proportional to magnetic pressure. This equation is quite general and allows any time variation of the magnetic field to be used. The equation of motion is termed the rocket equation, because, like a rocket, the mass decreases as the foil accelerates.

3.4 MASS EROSION COUPLED WITH MASS GRADING.

One important effect that must be considered is the effect of mass erosion coupled to the variation of magnetic pressure across the foil surface. Will mass erosion destroy the effects of mass grading?

The foil switch is based on one-dimensional motion; that is, it assumes the foil will move essentially as a flat sheet rather than distorting or bursting. In the geometry of the experiment, the magnetic field varies as $1/r$, and thus the magnetic pressure varies as $1/r^2$. The foil was also mass graded so that

$$\partial_t V = B^2/(8\pi\mu) = A(t) \quad ; \tag{3.45}$$

therefore, the whole foil should accelerate as a unit. This was confirmed by simulations of the experiment performed using the code AXFOIL,[7] which simulated the foil in two-dimensions as a collection of point masses. However, the mass grading presumed that μ would be constant in time. If μ varied in time by Equation 3.41a, would this cause even a mass-graded foil to be unstable and distort in two-dimensions?

We use V_c, the velocity for a constant μ ($V_c = W(t)/\mu_o$), and write

$$V(t) = \frac{V_c(t)}{(1 - KV_c(t))} \quad . \tag{3.46}$$

For the case of a mass-graded foil,

$$\partial_r V_c(t) = 0 \quad , \tag{3.47}$$

V_c is a constant in radius; that is, all the parts of the foil accelerate together, and accordingly,

$$\partial_r V(t) = 0 \quad . \tag{3.48}$$

Therefore, mass erosion at a rate proporational to acceleration, allows mass grading and thus one dimensional motion to be preserved.

3.5 APPROXIMATIONS AND PROBLEMS ASSOCIATED WITH MASS EROSION.

We have seen in this section that nonlinear magnetic diffusion and strong acceleration can combine to give a new picture of foil motion: a model where mass disappears and acceleration is much more rapid than expected. We have found the equations of motion for mass erosion show that this is consistent with mass grading to achieve one-dimensional motion. It must be pointed out, however, that this last statement is only approximately true. The scale lengths for magnetic diffusion will not change with mass grading, so that the implied approximation used to describe mass erosion,

that foil thickness is much greater than the diffusion scale lengths, may not be valid in the thinnest regions of a mass-graded foil.

We have another problem with the mass erosion effect that has been derived. The foil in the LANL foil switch experiment will erode completely before it reaches the gap if the erosion rates we have derived are correct. Also, the experimental data indicated a diffuse vapor passing through the gap, not a rapidly moving foil.

In order to have a complete and self-consistent picture to interpret the foil experimental results, a picture of events after mass erosion has destroyed the foil must be added. The model will be discussed in detail in the next section.

3.6 FOIL MOTION AFTER EROSION: THE SNOWPLOW EQUATION.

As we have seen, foil erosion can lead to a rocket-like acceleration. However, the mass erosion rate we have derived indicates that foils in many experiments will erode completely. According to Equation 3.44, this will give an infinite velocity at $\mu \approx 0$. This, obviously, does not occur. What will occur will be a "saturation" of the velocity at some high value with acceleration ending.

The exact process of this saturation is difficult to characterize in detail, however, it can be described qualitatively.

Before the foil mass becomes zero ($\mu=0$) the last remaining layer of foil will heat rapidly and explode. This will occur because the nonlinear diffusion process, while it can occur, actually prevents any portion of the foil from having a thermal energy density above $B^2/8\pi$, i.e., $Q \approx B^2/8\pi$. Once the advancing nonlinear wave reaches the front surface of the foil, however, the current will have no further place to diffuse. The remaining layer of foil must then heat until it explodes into vapor. This is what seems to occur in the LANL Foil Switch Experiment.

We will assume the vaporized foil will explode forward ahead of the magnetic field and fill the gap uniformly.

The vapor will be partly ionized and thus be a conductor. The magnetic field will advance through it like a shock wave. We can describe this mathematically by using Newton's law:

$$V\partial_t\mu + \mu\partial_t V = B^2/8\pi \quad . \tag{3.48}$$

$$\partial_t(\mu V) = B^2/8\pi \tag{3.49}$$

In this case we assume that material will be swept up by the shock and then diffuse through it after being brought up to speed. Therefore, we have the approximation

$$\partial_t\mu \gg \mu\partial_t V \quad . \tag{3.50}$$

We then have

$$V\partial_t\mu = B^2/8\pi \tag{3.51}$$

with

$$\partial_t\mu = \rho_v V \quad , \tag{3.52}$$

where ρ_v = the mass density of the exploded foil cloud. We can then solve for V using Equations 3.51 and 3.52:

$$V_s = \left[\frac{B^2}{\rho_v 8\pi}\right]^{1/2} \quad . \tag{3.53}$$

where V_s is "snowplow" velocity. The velocity "saturates". No longer is acceleration proportional to B^2. Instead, velocity has become proportional to magnetic field strength.

3.7 DISCUSSION.

In this section we have derived the equations of motion for light foils undergoing nonlinear magnetic diffusion and high acceleration. We saw how this could lead to mass erosion and rapid acceleration of the foil. This motion was described by the rocket equation. It was also found that foils could erode completely and explode during acceleration. The magnetic field then moving as a shock wave through the exploded material. This was described by the snowplow equation. In the next section the equations of motion will be used to define the EFS model of foil motion and apply the model to the LANL switch experiment.

SECTION 4
THE EFS MODEL OF FOIL MOTION

In the previous section, we discussed the chief physical phenomenon leading to the EFS model: the concentration of current in the foil into a thin sheet rather than its uniform spread over the foil thickness. In this section, we will discuss the EFS model and then apply it to interpret the results of the LANL experiment.

4.1 THE "ROCKET" AND "SNOWPLOW" PHASES OF EFS.

The EFS model predicts two phases of the foil motion in a foil experiment. The first phase can be termed the mass erosion or "rocket" phase, because the equation for foil motion resembles that of a rocket; for a prescribed thrust, the foil accelerates very rapidly, because its mass decreases in time at a rate proportional to the thrust. The second phase is termed the "snowplow"[8] phase, because the foil, being largely eroded, explodes forward and becomes a mixture of plasma, vapor, and liquid droplets in the remainder of the transmission line. The magnetic field moves through this exploded foil material like a shock wave.

In the first phase, the foil equation of motion will be of the form discussed in the previous section:

$$V_R = \frac{W(t)}{\mu_o(1 - K\frac{W(t)}{\mu_o})}, \tag{4.1}$$

where K = 21 gm/(cm^2 sec-bar), and

$$W(t) = \int \frac{B^2}{8\pi}(t)dt \tag{4.2}$$

In the second phase, a shock wave or snowplow phase, the velocity of the foil will, in effect, saturate. The foil is assumed to explode or disassemble into droplets and vapor. To describe this regime, we have the "snowplow" equation

$$V_s = \left[\frac{B^2}{\rho_v 8\pi}\right]^{1/2} \quad , \tag{4.3}$$

where ρ_v is the vapor mass density in the transmission line. We thus have expressions for the foil velocity before and after t_E, the foil explosion time. To complete the EFS model, we assume continuity of the functions for velocity and distance at $t = t_E$

$$V_R\ (t_E) = V_s(t_E) \tag{4.4}$$

These four equations form the EFS model of foil motion. We can now apply this model to the LANL foil switch experiment.

4.2 INTERPRETATION OF THE LANL FOIL SWITCH RESULTS.

The LANL switch experiment results were that the foil traveled a distance, X_f = 1.1cm, in a time, $t_f \approx 7\mu s$, and that its final velocity was approximately, $V_f = 3\times10^5$ cm/sec. We can infer also that the foil changed state during its acceleration, accelerating first as a solid object and then becoming a diffuse shock wave.

We wish to explain these results in terms of the EFS model. Since the LANL results are in terms of final distance and velocity we can conveniently compare the EFS model with experiment by integrating the EFS Equations 4.1 and 4.3 in time to obtain the total distance traveled.

We have then

$$X_f = \int_{t_E}^{t_f} V_s\ (t)\ dt + \int_0^{t_E} \frac{W(t)dt}{\mu_o\left(1-K\ \frac{W(t)}{\mu_o}\right)} \quad , \tag{4.5}$$

where X_f is the total distance to the gap and for the LANL experiment

$$W(t) = 5\times10^3 \text{ bars } (t-1/(2\omega) \sin(2\omega t)) \quad . \tag{4.6}$$

The shock velocity is given by

$$V_s(t) = V_f \frac{B(t)}{B(t_f)} \quad , \tag{4.7}$$

assuming a uniform foil debris density. At this point, we can insert our theoretical values of the erosion constant, K, and obtain t_E. Alternately, we can solve for t_E and K simultaneously and then compare the value of K obtained experimentally with that obtained from diffusion theory. Here we will solve for both K and t_E experimentally and compare K with the theoretical value.

We solve for the foil break-up time t_E and the mass erosion constant K by solving Equation 4.5 consistent with a matching of shock velocity to foil speed at breakup:

$$V_s(t_E) = \frac{1}{\left(\frac{\mu_o}{W(t_E)} - K\right)} \quad . \tag{4.8}$$

We can eliminate K and solve for t_E using Equation 4.8

$$X_f = \int_{t_E}^{t_f} V_s(t)\, dt + \int_0^{t_E} \frac{dt}{\left(\frac{\mu_o}{W(t)} - \frac{\mu_o}{W(t_E)} + \frac{1}{V_s(t_E)}\right)} \quad . \tag{4.9}$$

When Equation 4.18 is solved by iterations, it gives the value $t_E = 3.9\times10^{-6}$sec. The value of K obtained is then

$$K = 19\text{gm}/[\text{cm}^2 \text{ sec-bar}] \quad , \tag{4.10}$$

which is very close to the value calculated in the last section,

$$K = 21\text{gm}/[\text{cm}^2 \text{ sec-bar}] \quad . \tag{4.11}$$

The graph of velocity versus time for the foil is given in Figure 7. Therefore, the EFS model would seem to be a successful model for explaining the LANL foil switch results.

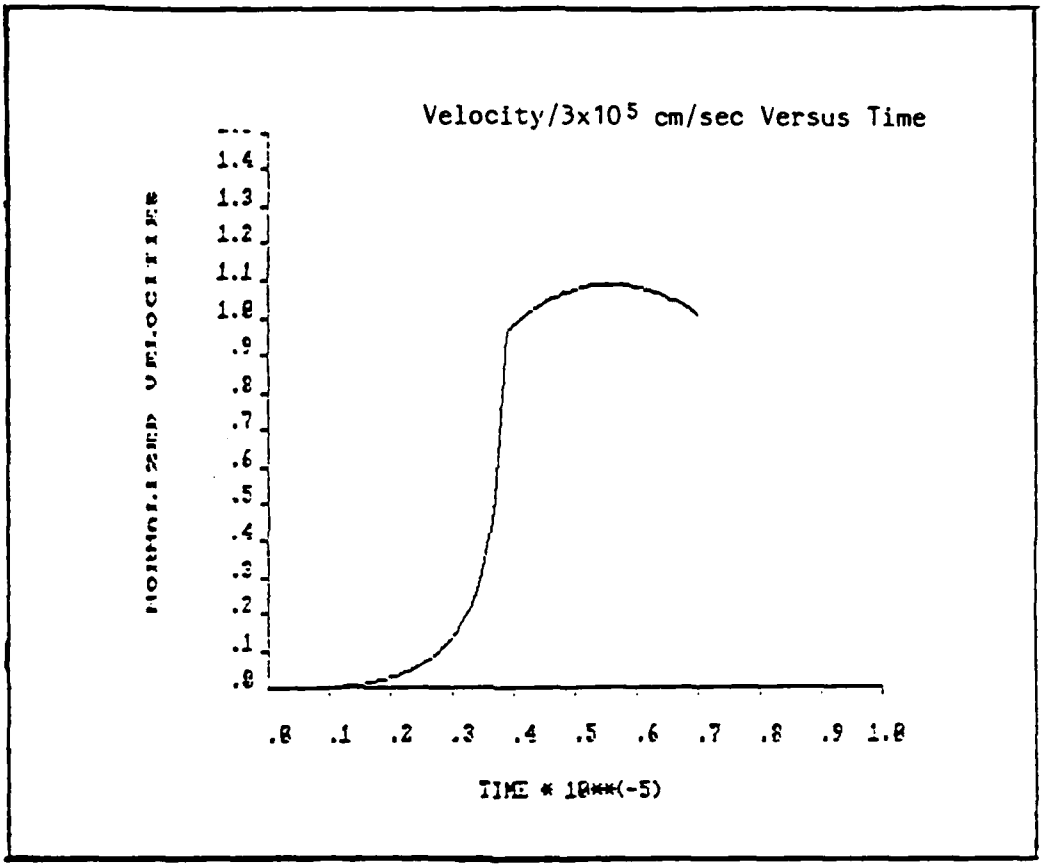

Figure 7. A plot of velocity versus time for the EFS model calculation of the Los Alamos foil switch experiment. Note that the sudden change in slope of the curve at 3.9 microseconds, the calculated foil explosion time. Time is given on the lower axis in 10^{-5} seconds.

SECTION 5
DISCUSSION AND SUMMARY

We have given a research report on the Eroding Foil Switch model. We have demonstrated that the EFS model is consistent with the picture of nonlinear magnetic diffusion. Highly stressed foils may have very nonuniform current distributions, rather than having a uniform current density and heating.

The fact that current is localized and moves through a foil as a thin layer, with an attendant localization of JXB forces and heating in a thin layer, means that the effective mass of the foil being pushed will decrease. It should be noted that this effect may be absent from more massive pieces of metal undergoing acceleration. If accelerations are small, metal behind the current layer will remain attached to the main mass of metal, and mass will not decrease. However, for the case of thin foils, mass erosion should be an an important effect.

The rate of mass loss per unit area was found to be

$$\partial_t \mu = -\rho_o V_B \tag{5.1}$$

$$V_B \propto B^2(t) \quad , \tag{5.2}$$

where ρ_o is the mass per unit area. This is an entirely reasonable scaling for mass loss, since it is proportional to the resistive heating rate. This leads to "rocket" equation of motion, because the foil mass decreases as it accelerates. The rate of erosion was also found to depend weakly on the frequency or rise time of the magnetic field, being faster for faster rise times.

A mass loss rate with this scaling is found to be consistent with stable acceleration of mass graded foils. The EFS model also suggests that foils which would be expected to remain solid during acceleration, using assumptions of uniform current, may be vaporized instead. In the case of total foil erosion the motion of the foil resembles a shock wave.

The shock wave speed is

$$V_s = B/(8\pi\rho_v)^{1/2} . \qquad (5.3)$$

This is very similar to a conventional shock wave speed with pressure being replaced by $B^2/8\pi$, the magnetic pressure. This is the "snowplow" phase of the motion, named from its simlarity to an MHD shock wave. This state may be thought of as a "saturation" of foil velocity, since acceleration ceases with the formation of the snowplow. The state of the foil material in the snowplow phase is more poorly defined than in the rocket phase. The only properties that can be inferred are low mass density and some electrical conductivity. More experimental data defining the foil state in this phase of motion are clearly required.

The EFS model suggests that the foil switch has great potential as a pulsed power tool. The model predicts that a foil can reach very high velocity yet have low temperature. The eroding material will be in the form of liquid or solid particles. Optimum switching may in fact occur before the foil erodes completely. This would allow a high speed foil to cross the gap leaving only a cloud of aluminum droplets in the gap.

In future reports, the EFS model will be applied to help interpret and optimize the results of upcoming experiments which will be conducted by Western Research Corporation.[9] The EFS model itself will be refined as experimental data becomes more abundant.

SECTION 6
LIST OF REFERENCES

1. D. R. Kania, et. al., Appl. Phys. Lett. (45) 26, 1984.

2. D. R. Kania, et. al., Appl. Phys. Lett. (44) 741, 1984.

3. J. E. Brandenburg, "Physical Properties and Mathematical Models of Foils in High Current Switches," Mission Research Corporation Report, MRC/WDC-R-106.

4. R. J. Trainor, Los Alamos National Laboratory, private communication.

5. Irvin R. Lendemuth, et. al., J. Appl. Phys. (57), p. 4447, (1985).

6. H. Knoepfel, "Pulsed High Magnetic Fields," North-Holland, New York, P. 93, (1970).

7. John Ambrosiano and J. E. Brandenburg, "AXFOIL: A Simple, Finite Element Computer Code to Model Moving Axial Foils," BRA-85-310R, Berkeley Research Associates Technical Report, July 1985.

8. Nicholas A. Krall and Alvin W. Trivelpiece, "Principles of Plasma Physics," McGraw-Hill, New York, p. 124, (1973).

9. Dr. Robert Miche, Western Research Corporation, private communication.

DISTRIBUTION LIST

DEPARTMENT OF DEFENSE

ASST TO THE SECY OF DEFENSE ATOMIC ENERGY
ATTN: EXECUTIVE ASSISTANT

DEFENSE INTELLIGENCE AGENCY
ATTN: DT-1B R RUBENSTEIN
ATTN: RTS-2B

DEFENSE NUCLEAR AGENCY
ATTN: RAAE
ATTN: RAEE
2 CYS ATTN: RAEV
ATTN: STNA
4 CYS ATTN: STTI-CA

DEFENSE TECHNICAL INFORMATION CENTER
12 CYS ATTN: DD

FIELD COMMAND DNA DET 2
LAWRENCE LIVERMORE NATIONAL LAB
ATTN: FC-1

FIELD COMMAND DEFENSE NUCLEAR AGENCY
ATTN: FCTT
ATTN: FCTT W SUMMA
ATTN: FCTXE

UNDER SECY OF DEF FOR RSCH & ENGRG
ATTN: STRAT & SPACE SYS (OS)

DEPARTMENT OF THE ARMY

HARRY DIAMOND LABORATORIES
ATTN: SCHLD-NW-P
ATTN: SLCHD-NW-RA
ATTN: SLCHD-NW-RI KERVIS 22900
ATTN: SLCIS-IM-TL 81100 TECH LIB

U S ARMY NUCLEAR & CHEMICAL AGENCY
ATTN: LIBRARY

U S ARMY TEST AND EVALUATION COMD
ATTN: AMSTE-

US ARMY MISSILE COMMAND
ATTN: REDSTONE SCI INFO CTR

DEPARTMENT OF THE NAVY

NAVAL RESEARCH LABORATORY
ATTN: CODE 2000 J BROWN
ATTN: CODE 4700 S OSSAKOW
ATTN: CODE 4701 I VITOKOVITSKY
ATTN: CODE 4720 J DAVIS
ATTN: CODE 4770 G COOPERSTEIN

NAVAL SURFACE WEAPONS CENTER
ATTN: CODE R40

NAVAL SURFACE WEAPONS CENTER
ATTN: CODE H-21

NAVAL WEAPONS CENTER
ATTN: CODE 343 FKA6A2 TECH SVCS

DEPARTMENT OF THE AIR FORCE

AIR FORCE WEAPONS LABORATORY, AFSC
ATTN: NT
ATTN: SUL

BALLISTIC MISSILE OFFICE/DAA
ATTN: ENSN

DEPUTY CHIEF OF STAFF/AF-RDQI
ATTN: AF/RDQI

SPACE DIVISION
ATTN: YNV

SPACE DIVISION/XR
ATTN: XR PLANS

SPACE DIVISION/YA
ATTN: YAR
ATTN: YAS

SPACE DIVISION/YE
ATTN: YEZ

SPACE DIVISION/YG
ATTN: YGJ

SPACE DIVISION/YK
ATTN: YFF

DEPARTMENT OF ENERGY

DEPARTMENT OF ENERGY
ATTN: OFC OF INERT FUSION
ATTN: OFC OF INERT FUSION C HILLAND
ATTN: OFC OF INERT FUSION R SHRIEVER

UNIVERSITY OF CALIFORNIA
LAWRENCE LIVERMORE NATIONAL LAB
ATTN: L-13 D MEEKER
ATTN: L-153

DEPARTMENT OF ENERGY (CONTINUED)

UNIVERSITY OF CALIFORNIA
LAWRENCE LIVERMORE NATIONAL LAB (CONTINUED)
ATTN: L-53 TECH INFO DEPT LIB
ATTN: L-545 J NUCKOLLS CLASS L-33

LOS ALAMOS NATIONAL LABORATORY
ATTN: B259 MS J BROWNELL

SANDIA NATIONAL LABORATORIES
ATTN: G W KUSWA ORG 1601
ATTN: J E POWELL 1230
ATTN: M J CLAUSER ORG 1271
ATTN: ORG 2312 D J ALLEN
ATTN: TECH LIB 3141

OTHER GOVERNMENT

CENTRAL INTELLIGENCE AGENCY
ATTN: OSWR/NED

DEPARTMENT OF DEFENSE CONTRACTORS

ADVANCED RESEARCH & APPLICATIONS CORP
ATTN: R ARMISTEAD

AEROSPACE CORP
ATTN: LIB ACQ M1/199
ATTN: V JOSEPHSON

BDM CORP
ATTN: CORPORATE LIB

BDM CORP
ATTN: L O HOEFT

EOS TECHNOLOGIES, INC
ATTN: B GABBARD

GENERAL ELECTRIC CO
ATTN: H O'DONNELL

IRT CORP
ATTN: N RUDIE
ATTN: R MERTZ

JAYCOR
ATTN: E WENAAS

JAYCOR
ATTN: R SULLIVAN

JAYCOR
ATTN: C ROGERS

KAMAN SCIENCES CORP
ATTN: S FACE

KAMAN SCIENCES CORP
ATTN: E CONRAD

KAMAN SCIENCES CORPORATION
ATTN: TECH LIB FOR D PIRIO

KAMAN TEMPO
ATTN: DASIAC

KAMAN TEMPO
ATTN: DASIAC

LOCKHEED MISSILES & SPACE CO, INC
ATTN: L CHASE

LOCKHEED MISSILES & SPACE CO, INC
ATTN: S TAIMUTY DEPT 81-74/154

MAXWELL LABS, INC
ATTN: A KOLB
ATTN: M MONTGOMERY

MCDONNELL DOUGLAS CORP
ATTN: S SCHNEIDER

MISSION RESEARCH CORP
2 CYS ATTN: J BRANDENBURG
2 CYS ATTN: R TERRY

MISSION RESEARCH CORP
ATTN: C LONGMIRE

MISSION RESEARCH CORP, SAN DIEGO
ATTN: V VAN LINT

PACIFIC-SIERRA RESEARCH CORP
ATTN: H BRODE, CHAIRMAN SAGE
ATTN: L SCHLESSINGER

PHYSICS INTERNATIONAL CO
ATTN: C GILMAN
ATTN: C STALLINGS
ATTN: G FRAZIER

PULSE SCIENCES, INC
ATTN: I D SMITH
ATTN: P W SPENCE
ATTN: S PUTNOM

R & D ASSOCIATES
ATTN: C KNOWLES

R & D ASSOCIATES
ATTN: P TURCHI

RAND CORP
ATTN: P DAVIS

RAND CORP
ATTN: B BENNETT

S-CUBED
ATTN: A WILSON

DEPT OF DEFENSE CONTRACTORS (CONTINUED)

SCIENCE APPLICATIONS INTL CORP
ATTN: K SITES

SCIENCE APPLICATIONS INTL CORP
ATTN: W CHADSEY

TRW ELECTRONICS & DEFENSE SECTOR
ATTN: D CLEMENT
ATTN: TECH INFO CTR,DOC ACQ

END

10-86

DTIC